MULTIPLE SCLEROSIS JOURNAL | MSJ

Original Research Paper

MRI correlates of clinical disability and hand-motor performance in multiple sclerosis phenotypes

Multiple Sclerosis Journal

1–17

DOI: 10.1177/1352458520958356

Claudio Cordani, Milagros Hidalgo de la Cruz, Alessandro Meani, Paola Valsasina, Federica Esposito, Elisabetta Pagani, Massimo Filippi and Maria A Rocca

Abstract

Background: Hand-motor impairment affects a large proportion of multiple sclerosis (MS) patients; however, its substrates are still poorly understood.

Objectives: To investigate the association between global disability, hand-motor impairment, and alterations in motor-relevant structural and functional magnetic resonance imaging (MRI) networks in MS patients with different clinical phenotypes.

Methods: One hundred thirty-four healthy controls (HC) and 364 MS patients (250 relapsing-remitting MS (RRMS) and 114 progressive MS (PMS)) underwent Expanded Disability Status Scale (EDSS) rating, nine-hole peg test (9HPT), and electronic finger tapping rate (EFTR). Structural and resting state (RS) functional MRI scans were used to perform a source-based morphometry on gray matter (GM) components, to analyze white matter (WM) tract diffusivity indices and to perform a RS seed-based approach from the primary motor cortex involved in hand movement (hand-motor cortex). Random forest analyses identified the predictors of clinical impairment.

Result: In RRMS, global measures of atrophy and lesions together with measures of structural damage of motor-related regions predicted EDSS (out-of-bag (OOB)-R^2 = 0.19, p-range = <0.001–0.04), z9HPT (right: OOB-R^2 = 0.14; left: OOB-R^2 = 0.24, p-range = <0.001–0.03). No RS functional connectivity (FC) abnormalities were identified in RRMS models. In PMS, cerebellar and sensorimotor regions atrophy, cerebellar peduncles integrity and increased RS FC between left hand-motor cortex and right inferior frontal gyrus predicted EDSS (OBB-R^2 = 0.16, p-range = 0.02–0.04).

Conclusion: In RRMS, only measures of structural damage contribute to explain motor impairment, whereas both structural and functional MRI measures predict clinical disability in PMS. A multiparametric MRI approach could be relevant to investigate hand-motor impairment in different MS phenotypes.

Keywords: Multiple sclerosis, magnetic resonance imaging, disability, hand-motor function, motor network

Date received: 14 May 2020; revised: 6 July 2020; accepted: 18 August 2020

Correspondence to:
MA Rocca
Neuroimaging Research Unit, Institute of Experimental Neurology, Division of Neuroscience, IRCCS San Raffaele Scientific Institute, Via Olgettina, 60 - 20132, Milan, Italy.
rocca.mara@hsr.it

Claudio Cordani
Milagros Hidalgo de la Cruz
Alessandro Meani
Paola Valsasina
Elisabetta Pagani
Neuroimaging Research Unit, Institute of Experimental Neurology, Division of Neuroscience, IRCCS San Raffaele Scientific Institute, Milan, Italy

Federica Esposito
Neurology Unit, IRCCS San Raffaele Scientific Institute, Milan, Italy

Massimo Filippi
Neuroimaging Research Unit, Institute of Experimental Neurology, Division of Neuroscience, IRCCS San Raffaele Scientific Institute, Milan, Italy/Neurology Unit, IRCCS San Raffaele Scientific Institute, Milan, Italy/Neurophysiology Unit, IRCCS San Raffaele Scientific Institute, Milan, Italy/Vita-Salute San Raffaele University, Milan, Italy

Maria A Rocca
Neuroimaging Research Unit, Institute of Experimental Neurology, Division of Neuroscience, IRCCS San Raffaele Scientific Institute, Milan, Italy/Neurology Unit, IRCCS San Raffaele Scientific Institute, Milan, Italy

Introduction

Upper limb motor impairment affects up to 60% of multiple sclerosis (MS) patients, having relevant effects on their functional independence, neuropsychological performance, and quality of life.[1] Impaired fine hand-motor dexterity, coordination deficits, and muscle weakness are the most frequent manifestations of upper limb impairment[2] and have a greater impact in the progressive phases of the disease.[1]

In daily clinical practice, the level of disability in MS patients is generally evaluated with the Expanded Disability Status Scale (EDSS),[3] a scale that mainly measures impairment of ambulation, particularly for values higher than 4. Functional scales more specific for the evaluation of hand-motor performance are rarely used. Among these, the nine-hole peg test (9HPT) measures fine hand-motor dexterity and coordination,[4,5] whereas the finger tapping rate test is sensible in identifying fine motor control.[6]

Interestingly, even if walking is the most frequent and relevant impaired function in MS patients, recent studies highlighted that worse 9HPT performances

have detrimental effects on daily life activities, like dressing or cooking[7]. This limitation is particularly present in progressive MS (PMS) patients, which, in many cases, show a bilateral overt impairment[8].

Studies using advanced magnetic resonance imaging (MRI) techniques are contributing to characterize the substrates associated with the different clinical manifestations of MS[9]. In particular, compared to relapsing-remitting (RR) MS, PMS patients seem to have higher gray matter (GM) loss in several regions of fronto-parieto-temporo-occipital lobes, cerebellum and deep GM structures[10], as well as more widespread microstructural white matter (WM) damage[11]. Through the analysis of resting state (RS) fMRI, complex patterns of decreased and increased RS functional connectivity (FC) have been attributed to the clinical manifestations of the main MS phenotypes[12]. Moreover, MS patients show different brain activations based on their disability level, also during simple motor tasks, with increased compensatory recruitment in early disease phases and deactivation, in advanced disease stages, of additional regions, which however can represent maladaptive processes[13].

Although recent studies have started to shed light on brain-motor regions contributing to hand-motor-performance in MS[14,15], the characterization of these aspects in the main MS phenotypes using multiparametric structural and functional MRI approaches is still lacking.

Against this background, we selected a large cohort of MS patients, and characterized, in MS patients versus healthy controls (HC) and in relapsing-remitting (RR) versus PMS patients: (1) atrophy of selected sensorimotor GM regions, (2) microstructural damage in motor-related WM tracts, and (3) RS FC abnormalities of the left- and right-hand motor-related networks. Then, multivariate analyses were used to investigate associations between the observed MRI abnormalities and global clinical disability (measured by EDSS), manual dexterity and coordination (measured by 9HPT), and fine motor control (measured by the electronic maximum finger tapping rate test, EFTR) impairment.

Subjects and methods

Ethics committee approval

This study was approved by the local ethical standards committee. Written informed consent was obtained from all participants.

Subjects and clinical assessment

From our unit database, we retrospectively selected 134 HC (71 female; median age = 38 years) and 364 sex- and age-matched MS patients (226 female; median age = 43 years; 250 RRMS and 114 PMS) satisfying the following inclusion criteria: right handedness (Edinburgh Handedness Inventory pre-MS condition 50); [16] no history of neurological (apart MS), orthopedic, or rheumatologic disorders; no psychiatric or mood disorders; no concomitant therapy with antidepressants, baclofen, psychoactive drugs or steroids; no drug or alcohol abuse. In addition, MS patients had to have: absence of relapses and steroid treatment in the 3 months preceding study enrollment, stable treatment for MS for at least 1 month, and no inclusion in a motor rehabilitation program in the previous 3 months.

All study subjects performed hand dexterity tests of both left and right hand using 9HPT and EFTR. In MS patients, a complete neurological examination, with rating of the EDSS score and recording of disease-modifying treatment (DMT), was also performed. Part of study subjects were previously analyzed[15].

MRI acquisition and conventional analysis

Details on acquisition and conventional MRI analysis are provided in Supplementary methods. Using a Philips Intera 3.0 Tesla scanner, the following brain sequences were acquired, during a single session: (1) dual-echo turbo-spin-echo (resolution = 0.94 × 0.94 × 3 mm^3) for T2-hyperintense lesion volume (LV) assessment; (2) three-dimensional (3D) T1-weighted scan (resolution = 0.89 × 0.89 × 0.9 mm^3) for T1-hypointense LV assessment and whole-brain and regional GM volume calculation; (3) diffusion-weighted sequence (resolution = 2.14 × 2.6 × 2.3 mm^3) for measuring WM microstructural alterations; and (4) T2*-weighted echo-planar-imaging sequence (resolution: 1.9 × 1.9 × 4 mm^3; 200 sets of 30 contiguous axial slices, with a 4 mm thickness) for RS FC assessment.

Source-based morphometry analysis

Source-based morphometry (SBM) post-processing is reported in detail in Supplementary methods. Preprocessed GM maps underwent SBM to produce GM components, that is, groups of spatially distinct GM regions showing common covariations among subjects. This was achieved using the GIFT SBM toolbox[17]. Visual inspection allowed to select GM components relevant for motor functions. Loading coefficients (Lc), representing the degree to which a

GM pattern is present at an individual level, were extracted and used for subsequent statistical analysis. When the main sign of the component was negative, GM map and *Lc* were inverted.[17]

Diffusion tensor MRI analysis

Diffusion tensor (DT) MRI analyses are detailed in Supplementary methods. Briefly, for each subject, fractional anisotropy (FA) and mean diffusivity (MD) maps were estimated using FSL (FDT tool, FSL 5.0.5). After standard space registration and skeletonization, average FA and MD values of corticospinal tracts, body of corpus callosum (CC), and cingulum, superior, middle, and inferior cerebellar peduncles were extracted and used for the analyses.

RS FC analysis

Details of RS fMRI pre-processing and seed-based RS FC analysis are reported in the Supplementary methods and in a previous publication.[18] Briefly, RS FC maps of the left- and right-hand motor cortex were produced by seed-based correlation analysis. Seeds for RS FC were identified starting from the primary motor cortices involved in hand movement (hand-motor cortices, identifiable by the omega-shape knobs) on 3D T1-weighted scans, and shifted to match the closest peak of activation within the functional sensorimotor system, identified by independent component analysis (GIFT software).

Demographic and clinical variables analysis

Demographic and clinical variables were compared between MS patients and HC, and between MS phenotypes using the Mann–Whitney *U* test and chi-square test as appropriate. Linear models in the HC group were applied to regress out the effect of age and sex on inverse 9HPT and EFTR scores.[6] The residuals (difference between the observed and predicted values) for both HC and MS patients were then converted to *z*-scores (z9HPT and zEFTR), using the standard deviation of HC residuals, and compared by linear models for heteroscedastic data. The following a priori comparisons were defined, based on the clinical evolution of the disease: (1) RRMS patients versus HC and (2) PMS versus RRMS patients.

MRI analyses

Differences of right- and left-hand motor RS FC between MS patients and HC were assessed using SPM12 and age- and sex-adjusted linear models. Average right- and left-hand RS FC maps of the whole group were used as masks. Results were assessed at a threshold of $p < 0.05$, family-wise-error corrected for multiple comparisons and also tested at a $p < 0.001$, uncorrected (cluster extension, kE = 5). The mean RS FC Z-scores of clusters significant at the previous comparison were extracted using the *MarsBaR* toolbox (http://marsbar.sourceforge.net/) and used for subsequent analyses.

LVs were log-transformed to reduce skewness. Between-group comparisons of MRI measures were performed applying age- and sex-adjusted linear models for heteroscedastic data, allowing for group-specific error variances, and expressed in terms of effect size, a standardized score computed as the ratio between estimated differences and the HC error term. Results were assessed at $p < 0.05$ accounting for the number of tested comparisons using the false discovery rate approach.[19]

Random forest analyses

Random forest regression models[20] (*R* software, version 3.6.3, *ranger* package) were performed to identify conventional and motor-related MRI variables (those significantly different in MS vs HC) associated with global disability and impaired hand performance in: (1) all MS, (2) RRMS, and (3) PMS patients. Demographic and clinical variables were included in the analyses. For each model, 10,000 regression trees were built on a random subset of covariates, with a 0.632+ bootstrap resampling of the observations.[21] According to Altmann et al.,[22] a permutation test (1000 permutations) of the outcome was applied to assess the feature relevance, providing a corrected measure of variable importance and significance *p*-values for each predictor. The goodness of fit of a new model, trained using only the selected predictors ($p < 0.05$), was expressed by the out-of-bag (OOB)-R^2, the coefficient of multiple determination computed on the left-out observations.

Results

Demographic and clinical characteristics

The main demographic and clinical characteristics of the study participants are reported in Table 1. Compared to HC, MS patients showed significantly higher hand-motor impairment, measured as lower scores in z9HPT and zEFTR of both hands ($p < 0.001$). As expected, compared to RRMS, PMS patients were older, had higher EDSS score, longer disease duration, and more severe motor impairment ($p < 0.001$, for all comparisons). RRMS and PMS significantly

Table 1. Main demographic and clinical characteristics of healthy controls (HC) and multiple sclerosis (MS) patients.

Variable	HC ($n=134$)	MS ($n=364$)	RRMS ($n=250$)	PMS ($n=114$)	MS vs HC	RRMS vs HC	PMS vs RRMS
Sex (male/female)	63/71	138/226	93/157	45/69	0.07[a]	0.06[a]	0.68[a]
Median age (years) (IQR)	38.0 (30.9–50.2)	43.1 (33.4–50.8)	39.2 (29.1–46.8)	50.4 (43.8–57.0)	0.09[b]	0.21[b]	**<0.001**[b]
Median EHI % (IQR)	91 (82–100)	84 (75–100)	85 (76–100)	82.5 (75–100)	0.13[b]	0.27[b]	0.86[b]
Median EDSS (IQR)	–	2.5 (1.5–5.5)	1.5 (1.0–2.5)	6.0 (5.5–6.5)	–	–	**<0.001**[b]
Median disease duration (years) (IQR)	–	12.7 (7.0–18.9)	10.2 (5.8–16.0)	16.8 (13.0–25.0)	–	–	**<0.001**[b]
Median right 9HPT (seconds) (IQR)	18.4 (17.1–21.3)	24.3 (21.0–30.0)	22.0 (20.0–25.1)	31.4 (27.1–44.1)	**<0.001**[c]	**<0.001**[c]	**<0.001**[c]
Mean right z9HPT (SD)	0 (1.0)	−1.61 (1.22)	−1.16 (0.97)	−2.59 (1.12)			
Median left 9HPT (seconds) (IQR)	20.2 (18.5–22.4)	26.0 (22.4–31.5)	24.0 (21.6–28.0)	34.1 (28.0–39.9)	**<0.001**[c]	**<0.001**[c]	**<0.001**[c]
Mean left z9HPT (SD)	0 (1.0)	−1.59 (1.26)	−1.15 (1.03)	−2.54 (1.19)			
Median right EFTR (taps in 30 seconds) (IQR)	131 (115–147)	105 (80–124)	115 (97–133)	79 (56–100)	**<0.001**[c]	**<0.001**[c]	**<0.001**[c]
Mean right zEFTR (SD)	0 (1.0)	−1.14 (1.45)	−0.69 (1.31)	−2.22 (1.18)			
Median left EFTR (taps in 30 seconds) (IQR)	123 (108–134)	98 (78–116)	107 (91–121)	78 (58–93)	**<0.001**[c]	**<0.001**[c]	**<0.001**[c]
Mean left zEFTR (SD)	0 (1.0)	−1.18 (1.38)	−0.76 (1.24)	−2.10 (1.25)			
DMT[d] (none/first line/second line)	–	51/179/134	11/147/92	40/32/42	–	–	**<0.001**[a]

HC: healthy controls; MS: multiple sclerosis; RRMS: relapsing-remitting MS; PMS: progressive MS; SD: standard deviation; IQR: interquartile range; EHI: Edinburg Handedness Index; EDSS: Expanded Disability Status Scale; 9HPT: nine-hole peg test; EFTR: electronic finger tapping rate test; DMT: disease-modifying treatment.
Statistically significant results are highlighted in **bold**.
[a]Chi-square test.
[b]Mann–Whitney test.
[c]Linear models.
[d]First line: glatiramer acetate ($n=66$), interferon beta-1a/1b ($n=110$), teriflunomide ($n=3$); second-line drugs/immunosuppressants: azathioprine ($n=14$), cyclophosphamide ($n=10$), fingolimod ($n=60$), methotrexate ($n=5$), mitoxantrone ($n=1$), natalizumab ($n=41$), rituximab ($n=3$).

differed also for DMT-characteristics, with the majority of RRMS receiving either a first- or second-line DMT, whereas 35% of PMS received no treatment at study inclusion.

Conventional MRI findings

The main conventional MRI findings are shown in Table 2.

Compared to HC, MS patients had lower brain, GM and WM volumes ($p < 0.001$, for all comparisons). Compared to RRMS, PMS patients had higher T2-LV ($p = 0.005$), higher T1-LV ($p = 0.04$), and lower NBV ($p = 0.02$) and NGMV ($p = 0.04$).

SBM analysis

Nine GM components were selected and classified into three categories according to the cortical/subcortical areas mainly involved: four sensorimotor GM components (I–IV), four cerebellar GM components (I–IV), and one basal ganglia GM component (Figure 1). Compared to HC, MS patients showed significant GM atrophy (expressed as lower GM *Lc*) in all components (p range: <0.001–0.01), except for the cerebellar GM component II ($p = 0.06$). Compared to HC, RRMS patients showed GM atrophy in all components (p range: <0.001–0.04), except for cerebellar component III. Compared to RRMS, PMS showed atrophy in basal ganglia and cerebellar GM components I, III, and IV (p range: <0.001–0.04) (Table 2).

DTI analysis

Compared to HC, MS patients had reduced FA and increased MD in all WM tracts considered (Figure 1) (p range: <0.001–0.01). Similar results were found in RRMS versus HC, except for superior cerebellar peduncle FA (right: $p = 0.06$; left: $p = 0.21$). Compared to RRMS, PMS patients had more severe damage in all analyzed WM tracts, except for left superior cerebellar peduncles MD ($p = 0.07$) (Table 2).

RS FC analysis

Figure 2 shows left- and right-hand RS FC maps of the whole sample. The comparison between HC and MS patients demonstrated both increased and decreased RS FC between left- and right-hand motor cortices and many regions associated with sensorimotor and visuospatial functions (Figure 2, Table 3). Similar results were observed in RRMS versus HC. Compared to RRMS, PMS patients had reduced RS FC between the left-hand motor cortex and the right supplementary motor area, left hippocampal region, occipital areas, putamen, and postcentral gyrus (p range $= 0.001$–0.05). They also had reduced RS FC between the right-hand motor cortex and right precuneus and left cerebellum crus II ($p = 0.04$, for both areas) (Table 3).

Random forest analysis

Whole MS sample. Table 4 and Figure 3 summarize the results of random forest analyses in the whole MS sample. In MS patients, the most relevant predictors of EDSS score (OOB-$R^2 = 0.71$) among those selected by the model were (in order of importance, first five listed) NBV, NGMV, atrophy of the cerebellar GM component I, right inferior cerebellar peduncle FA, and atrophy of basal ganglia GM component. Best predictors of right z9HPT performance (OOB-$R^2 = 0.36$) were right inferior cerebellar peduncle FA, NBV, NGMV, atrophy of cerebellar GM component III, and right inferior cerebellar peduncle MD. Best predictors of left z9HPT performance (OOB-$R^2 = 0.38$) were T1-LV, left inferior cerebellar peduncle FA, T2-LV, NBV, and CC-body FA.

Best predictors of right-zEFTR performance (OOB-$R^2 = 0.18$) were NGMV, atrophy of sensorimotor and cerebellar GM components I and IV and right inferior cerebellar peduncle MD. Finally, left-zEFTR predictors (OOB-$R^2 = 0.22$) were left inferior and middle cerebellar peduncles FA, NGMV, as well as atrophy of cerebellar and sensorimotor GM components (IV and I, respectively).

MS phenotypes

Results in MS phenotypes are summarized in Table 5. In RRMS patients, EDSS was mainly predicted (OOB-$R^2 = 0.19$) by atrophy of basal ganglia GM component, NBV, NGMV, CC-body MD, and CC-body FA.

Best predictors of right z9HPT performance (OOB-$R^2 = 0.14$) were NGMV, T2-LV, left cingulum FA, NBV, and right inferior cerebellar peduncle FA. Best predictors of left z9HPT performance (OOB-$R^2 = 0.24$) were left inferior cerebellar peduncle FA, T1-LV, atrophy of basal ganglia GM component, T2-LV, and CC-body MD. No predictors of right and left zEFTR performance were found.

In PMS patients, significant predictors were observed only linked to EDSS score (OOB-$R^2 = 0.16$) and were atrophy of cerebellar GM component I and sensorimotor GM component II, left inferior cerebellar

Table 2. Conventional MRI measures, loading coefficients (*Lc*) of gray matter network components (calculated with source-based morphometry analysis) and diffusion tensor indices in the considered white matter tracts ($p < 0.05$, FDR corrected), in healthy controls (HC) and multiple sclerosis (MS) patients.

Variable	HC ($n=134$) Mean (SD)	MS ($n=364$) Mean (SD)	RRMS ($n=250$) Mean (SD)	PMS ($n=114$) Mean (SD)	MS vs HC ES (p_{FDR})	RRMS vs HC ES (p_{FDR})	PMS vs RRMS ES (p_{FDR})
Conventional MRI measures							
T2-LV (mL)	0.41 (0–0.49)[a]	5.60 (2.66–12.03)[a]	4.64 (2.21–9.33)[a]	8.71 (4.18–20.92)[a]	– (**<0.001**)	– (**<0.001**)	0.39[b] (**0.005**)
T1-LV (mL)	0.27 (0–0.31)[a]	3.48 (1.38–8.32)[a]	2.59 (1.24–6.09)[a]	5.61 (2.48–15.18)[a]	– (**<0.001**)	– (**<0.001**)	0.28[b] (**0.04**)
Normalized brain volume (mL)	1585 (86)	1497 (110)	1522 (86)	1442 (95)	−1.09 (**<0.001**)	−0.98 (**<0.001**)	−0.44 (**0.02**)
Normalized GM volume (mL)	746 (60)	682 (78)	699 (73)	642 (64)	−1.41 (**<0.001**)	−1.29 (**<0.001**)	−0.44 (**0.04**)
Normalized WM volume (mL)	840 (42)	815 (50)	822 (42)	801 (51)	−0.49 (**<0.001**)	−0.42 (**<0.001**)	−0.27 (0.08)
Source-based morphometry measures							
Sensorimotor GM component I (*Lc*)	0.50 (0.88)	−0.21 (0.92)	−0.08 (0.94)	−0.50 (0.82)	−0.72 (**<0.001**)	−0.68 (**<0.001**)	−0.15 (0.27)
Sensorimotor GM component II (*Lc*)	0.46 (1.03)	−0.19 (0.93)	−0.05 (0.97)	−0.48 (0.77)	−0.52 (**<0.001**)	−0.50 (**<0.001**)	−0.11 (0.38)
Sensorimotor GM component III (*Lc*)	0.53 (0.85)	−0.24 (0.91)	−0.06 (0.91)	−0.63 (0.79)	−0.84 (**<0.001**)	−0.79 (**<0.001**)	−0.20 (0.18)
Sensorimotor GM component IV (*Lc*)	0.25 (0.89)	−0.16 (0.91)	−0.04 (0.91)	−0.42 (0.84)	−0.31 (**0.003**)	−0.33 (**0.005**)	0.06 (0.69)
Cerebellar GM component I (*Lc*)	0.33 (1.00)	−0.17 (0.93)	0.05 (0.89)	−0.65 (0.83)	−0.36 (**<0.001**)	−0.26 (**0.02**)	−0.35 (**0.007**)
Cerebellar GM component II (*Lc*)	0.21 (0.94)	−0.10 (0.92)	−0.06 (0.93)	−0.19 (0.90)	−0.19 (0.06)	−0.22 (**0.04**)	0.12 (0.31)
Cerebellar GM component III (*Lc*)	0.31 (0.91)	−0.11 (0.98)	0.08 (0.91)	−0.53 (1.00)	−0.27 (**0.01**)	−0.19 (0.10)	−0.32 (**0.04**)
Cerebellar GM component IV (*Lc*)	0.35 (0.99)	−0.15 (0.95)	0.09 (0.90)	−0.68 (0.83)	−0.34 (**0.001**)	−0.22 (**0.04**)	−0.44 (**<0.001**)
Basal ganglia GM component (*Lc*)	0.64 (0.68)	−0.27 (0.98)	−0.07 (0.94)	−0.70 (0.95)	−1.35 (**<0.001**)	−1.20 (**<0.001**)	−0.57 (**0.007**)
Diffusion tensor imaging measures							
Left corticospinal tract FA	0.62 (0.02)	0.61 (0.02)	0.61 (0.02)	0.60 (0.02)	−0.78 (**<0.001**)	−0.70 (**<0.001**)	−0.32 (**0.03**)
Right corticospinal tract FA	0.62 (0.02)	0.60 (0.03)	0.60 (0.02)	0.59 (0.02)	−0.64 (**<0.001**)	−0.52 (**<0.001**)	−0.45 (**0.001**)
Left superior cerebellar peduncle FA	0.67 (0.03)	0.66 (0.03)	0.66 (0.04)	0.66 (0.04)	−0.28 (**0.01**)	−0.15 (0.21)	−0.52 (**0.001**)
Right superior cerebellar peduncle FA	0.66 (0.04)	0.65 (0.04)	0.66 (0.04)	0.65 (0.04)	−0.38 (**<0.001**)	−0.22 (0.06)	−0.63 (**<0.001**)
Left middle cerebellar peduncle FA	0.60 (0.02)	0.58 (0.03)	0.58 (0.03)	0.56 (0.03)	−1.04 (**<0.001**)	−0.88 (**<0.001**)	−0.59 (**0.002**)
Right middle cerebellar peduncle FA	0.60 (0.02)	0.57 (0.03)	0.58 (0.03)	0.56 (0.03)	−0.96 (**<0.001**)	−0.83 (**<0.001**)	−0.50 (**0.003**)
Left inferior cerebellar peduncle FA	0.57 (0.03)	0.54 (0.04)	0.55 (0.04)	0.53 (0.04)	−0.90 (**<0.001**)	−0.73 (**<0.001**)	−0.63 (**<0.001**)

(Continued)

Table 2. (Continued)

Variable	HC ($n=134$) Mean (SD)	MS ($n=364$) Mean (SD)	RRMS ($n=250$) Mean (SD)	PMS ($n=114$) Mean (SD)	MS vs HC ES (p_{FDR})	RRMS vs HC ES (p_{FDR})	PMS vs RRMS ES (p_{FDR})
Right inferior cerebellar peduncle FA	0.57 (0.03)	0.54 (0.04)	0.55 (0.04)	0.52 (0.04)	−0.95 (**<0.001**)	−0.77 (**<0.001**)	−0.71 (**<0.001**)
Left cingulum FA	0.60 (0.03)	0.57 (0.05)	0.58 (0.03)	0.56 (0.04)	−0.94 (**<0.001**)	−0.81 (**<0.001**)	−0.47 (**0.03**)
Right cingulum FA	0.58 (0.03)	0.54 (0.05)	0.55 (0.04)	0.53 (0.05)	−1.10 (**<0.001**)	−0.92 (**<0.001**)	−0.67 (**0.002**)
Corpus callosum body FA	0.70 (0.02)	0.64 (0.06)	0.65 (0.06)	0.62 (0.07)	−2.70 (**<0.001**)	−2.44 (**<0.001**)	−0.91 (**0.009**)
Left corticospinal tract MD ($mm^2/s \times 10^{-3}$)	0.72 (0.02)	0.73 (0.03)	0.73 (0.03)	0.74 (0.03)	0.73 (**<0.001**)	0.61 (**<0.001**)	0.46 (**0.02**)
Right corticospinal tract MD ($mm^2/s \times 10^{-3}$)	0.73 (0.02)	0.75 (0.03)	0.75 (0.03)	0.76 (0.03)	0.71 (**<0.001**)	0.56 (**<0.001**)	0.59 (**0.002**)
Left superior cerebellar peduncle MD ($mm^2/s \times 10^{-3}$)	0.84 (0.04)	0.85 (0.05)	0.85 (0.05)	0.85 (0.05)	0.37 (**<0.001**)	0.30 (**0.02**)	0.28 (0.07)
Right superior cerebellar peduncle MD ($mm^2/s \times 10^{-3}$)	0.85 (0.04)	0.87 (0.05)	0.87 (0.05)	0.88 (0.06)	0.44 (**<0.001**)	0.34 (**0.006**)	0.38 (**0.02**)
Left middle cerebellar peduncle MD ($mm^2/s \times 10^{-3}$)	0.74 (0.03)	0.75 (0.04)	0.75 (0.03)	0.75 (0.04)	0.52 (**<0.001**)	0.36 (**0.006**)	0.58 (**0.002**)
Right middle cerebellar peduncle MD ($mm^2/s \times 10^{-3}$)	0.74 (0.03)	0.75 (0.04)	0.75 (0.04)	0.76 (0.04)	0.56 (**<0.001**)	0.39 (**0.002**)	0.63 (**<0.001**)
Left inferior cerebellar peduncle MD ($mm^2/s \times 10^{-3}$)	0.77 (0.03)	0.78 (0.04)	0.78 (0.04)	0.78 (0.04)	0.47 (**<0.001**)	0.35 (**0.004**)	0.42 (**0.01**)
Right inferior cerebellar peduncle MD ($mm^2/s \times 10^{-3}$)	0.76 (0.03)	0.77 (0.04)	0.77 (0.03)	0.78 (0.04)	0.60 (**<0.001**)	0.41 (**0.001**)	0.68 (**<0.001**)
Left cingulum MD ($mm^2/s \times 10^{-3}$)	0.75 (0.03)	0.76 (0.04)	0.76 (0.03)	0.77 (0.04)	0.56 (**<0.001**)	0.44 (**<0.001**)	0.42 (**0.02**)
Right cingulum MD ($mm^2/s \times 10^{-3}$)	0.74 (0.03)	0.76 (0.04)	0.75 (0.03)	0.76 (0.04)	0.68 (**<0.001**)	0.50 (**<0.001**)	0.65 (**0.001**)
Corpus callosum body MD ($mm^2/s \times 10^{-3}$)	0.81 (0.03)	0.89 (0.09)	0.88 (0.09)	0.92 (0.09)	2.51 (**<0.001**)	2.24 (**<0.001**)	0.93 (**0.008**)

HC: healthy controls; MS: multiple sclerosis; RRMS: relapsing-remitting MS; PMS: progressive MS; SD: standard deviation; ES: effect size; FDR: false discovery rate; MRI: magnetic resonance imaging; GM: gray matter; *Lc*: loading coefficient; FA: fractional anisotropy; MD: mean diffusivity; LV: lesion volume; WM: white matter.
Statistically significant results are highlighted in **bold**.
[a]Data presented as median and interquartile range.
[b]ES computed dividing the estimated difference between phenotype and the pooled error term.

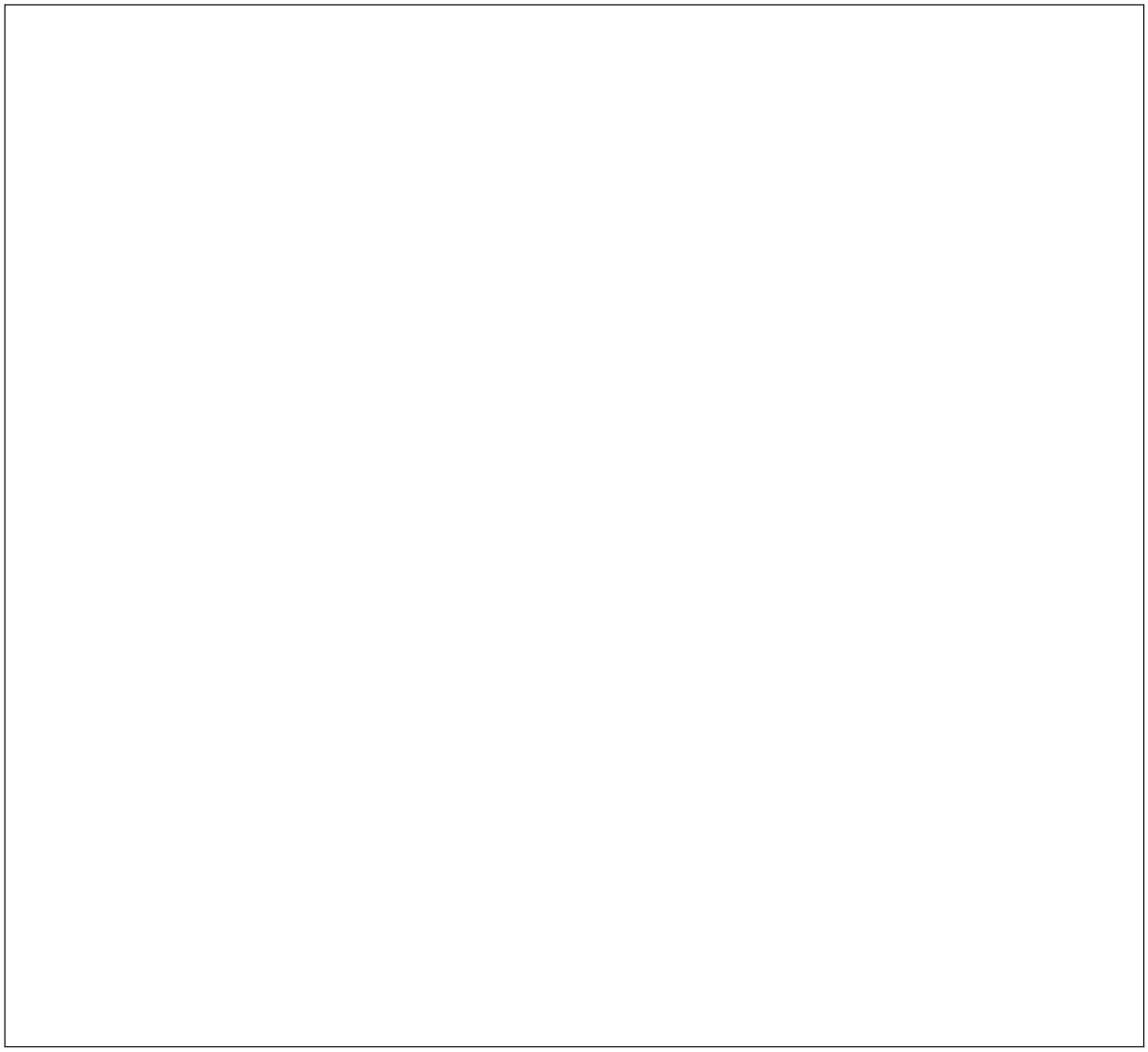

Figure 1. Motor-related gray matter components identified with source-based morphometry and white matter tracts selected from the atlas.
Composite map of the nine relevant independent components (ICs) after the selection procedure (see text for further details), sorted into three subcategories: (A) sensorimotor (four components), (B) cerebellar (four components), and (C) basal ganglia (one component). (D) White matter tract atlas from which mean factional anisotropy and mean diffusivity values of relevant-motor tracts (Red: cingulum and external capsule; blue-scale: corpus callosum; red-yellow: internal capsule; yellow: superior cerebellar peduncles; black: middle cerebellar peduncles; green: inferior cerebellar peduncles) were extracted. Images are presented in neurological convention. IC: independent component; L: left; R: right; P: posterior; A: anterior.

peduncle FA, and increased RS FC between left-hand motor cortex and inferior frontal gyrus (IFG).

Discussion

In this study, we applied a multimodal MRI approach to investigate the contribution of structural and functional damage in motor-related areas to global clinical disability and hand-motor impairment in a large group of MS patients. Differently from a previous study, in which we analyzed large portions of central nervous system (CNS) by applying non-hypothesis-driven voxel-based methods in a large group of MS patients,[15] here we performed an a priori selection of motor-related areas. In addition, we did not limit the analysis to MS patients as a whole, but also considered findings in RRMS and PMS patients, separately, to explore whether the mechanisms leading to global and hand-motor impairment differ over the course of the diseases. Finally, we also included the EFTR to broaden hand-motor performance assessment.

In line with the literature,[11,12,23,24] compared to HC, MS patients showed widespread brain damage, both

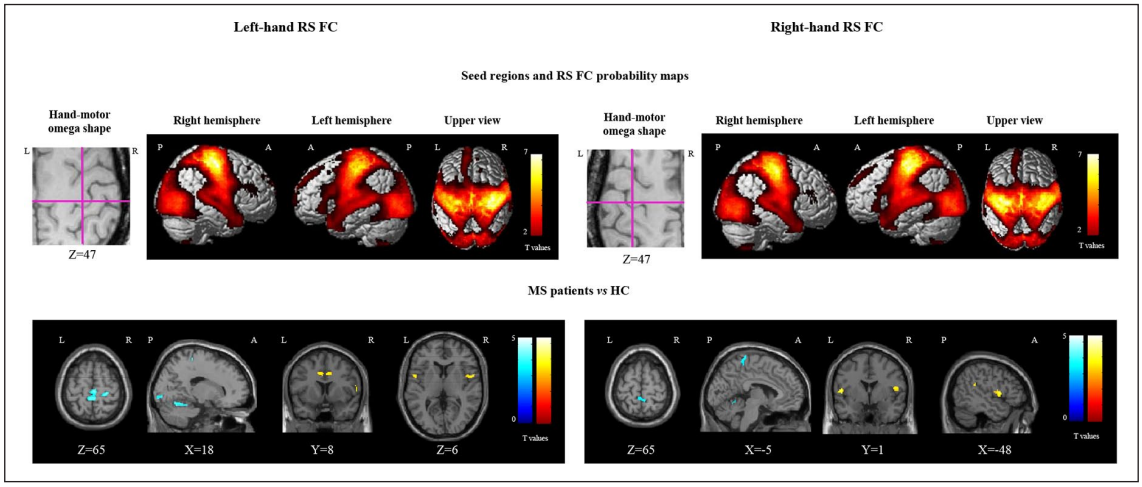

Figure 2. Resting state functional connectivity seed-based approach and differences between multiple sclerosis patients and healthy controls.
First row: seed regions on 3DT1-weighted images and left- and right-hand resting state (RS) functional connectivity (FC) probability maps (SPM12, one-sample, $p < 0.05$, family-wise error corrected for multiple comparison, cluster extent = 5; t values encoded in red-yellow). Second row: differences in left- and right-hand motor cortex RS FC between multiple sclerosis (MS) patients and healthy controls (HC) (SPM12, age- and sex-adjusted linear models, $p < 0.001$ uncorrected, cluster extent = 5; t values encoded in red-yellow for increased and in blue-light blue for reduced left- and right-hand motor cortex RS FC). Images are presented in neurological convention. See text for further details.
RS: resting state; FC: functional connectivity; L: left; R: right; P: posterior; A: anterior; MS: multiple sclerosis; HC: healthy controls.

at global level, in terms of measures of LV and atrophy, and at regional level, in terms of atrophy, WM microstructural alterations, and RS FC abnormalities in the majority of motor-related areas and networks analyzed. Such a widespread damage was already detectable in RRMS patients and became more significant in PMS patients, confirming that these typical features of MS pathology occur with different grades across the main stages of the disease.[11,12,23,24]

In RRMS patients, random forest analyses identified as predictors of clinical impairment (both global clinical disability and hand-motor impairment) several structural MRI measures of global CNS damage and of injury to motor-related areas, indicating that in this phenotype both the global amount of structural CNS damage and the involvement of clinically relevant areas/networks contribute to explain the severity of disease clinical manifestations. At global level, whole-brain and GM atrophy as well as focal WM lesions (T2- and T1-LV) confirm that widespread structural damage and irreversible tissue loss are associated with more severe clinical and motor disability in MS.[11] At regional level, a significant contribution of structural damage of the cerebellum was detected, both in terms of GM atrophy and cerebellar peduncle integrity. The cerebellum has a well-known role in motor performance, contributing not only to postural control[25] but also to sensorimotor integration and movement coordination, which are fundamental especially for hand-dexterity tasks.[15] Using DT MRI, previous studies have shown that part of MS clinical manifestations are related to damage to cerebellar WM tracts, probably as a consequence of a disconnection between the cerebellum and the cerebral hemispheres.[23] Not unexpectedly, EDSS and hand-motor impairment were also predicted by atrophy of basal ganglia component and structural integrity of the CC. By definition, these structures participate to different aspects of motor performance. The basal ganglia are involved in movement selection and timing,[15,26] while CC integrity has been associated with inter-manual motor function in patients with MS.[27] Of note, for none of the outcome clinical measures, random forest analysis identified measures derived from the analysis of RS FC of the hand-motor networks among the predictors. Such technique might be scarcely informative due to the wide variety of clinical manifestations which characterize this phenotype and for the high heterogeneity in RS FC modifications which these patients could experience in order to compensate the brain structural damage and disability accumulation.

The identification of the MRI correlates of motor impairment in RRMS patients is of fundamental importance because it may help to identify biomarkers which can guide medical and rehabilitative interventions, in a phase in which disability can be partially reversible.[28] In line with this, we were able to classify and rank in order of relative importance not

Table 3. Comparison of resting state (RS) functional connectivity (FC) in significant clusters (SPM12, $p < 0.001$, uncorrected; cluster extension (kE) = 5) of right- and left-hand motor networks between healthy controls (HC) and multiple sclerosis (MS) patients.

Region	MNI coordinates	kE	*T* value	HC Mean (SD)	MS Mean (SD)	RRMS Mean (SD)	PMS Mean (SD)	MS vs HC ES (p_{FDR})	RRMS vs HC ES (p_{FDR})	PMS vs RRMS ES (p_{FDR})
Reduced RS FC in MS vs HC										
Left-hand motor network										
Left precuneus	−2, −40, 68	377	4.77*	0.35 (0.26)	0.24 (0.20)	0.26 (0.20)	0.19 (0.19)	−0.38 (**<0.001**)	−0.32 (**0.003**)	−0.29 (**0.004**)
Right supplementary motor area	4, −24, 62		4.13*							
Right paracentral lobule	10, −34, 72		3.22*							
Left calcarine sulcus	−18, −50, 6	64	4.8	0.17 (0.21)	0.08 (0.17)	0.09 (0.17)	0.06 (0.16)	−0.39 (**<0.001**)	−0.36 (**0.001**)	−0.13 (0.21)
Left lingual gyrus	−22, −48, −2		3.37							
Right postcentral gyrus	28, −28, 60	65	4.23	0.57 (0.31)	0.41 (0.28)	0.42 (0.28)	0.40 (0.28)	−0.40 (**<0.001**)	−0.42 (**<0.001**)	0.07 (0.55)
Left parahippocampal gyrus	−28, −36, −6	22	4.21	0.21 (0.21)	0.12 (0.18)	0.14 (0.18)	0.07 (0.16)	−0.36 (**<0.001**)	−0.30 (**0.007**)	−0.25 (**0.01**)
Left hippocampus	−32, −30, −12		3.39							
Right fusiform gyrus	34, −42, −20	161	4.06	0.09 (0.15)	0.02 (0.15)	0.02 (0.15)	0.02 (0.14)	−0.44 (**<0.001**)	−0.46 (**<0.001**)	0.08 (0.49)
Left cerebellar lobule 4–5	−8, −46, −18	10	4.01	0.25 (0.28)	0.13 (0.23)	0.15 (0.22)	0.08 (0.23)	−0.33 (**<0.001**)	−0.31 (**0.004**)	−0.11 (0.27)
Left putamen	−20, 22, 4	79	3.91	0.08 (0.11)	0.02 (0.13)	0.03 (0.11)	0.002 (0.15)	−0.57 (**<0.001**)	−0.49 (**<0.001**)	−0.33 (**0.046**)
Left postcentral gyrus	−30, −34, 74	43	3.91	0.14 (0.18)	0.07 (0.17)	0.09 (0.17)	0.05 (0.15)	−0.35 (**<0.001**)	−0.29 (**0.01**)	−0.23 (**0.04**)
Left fusiform gyrus	−38, −52, −8	30	3.88	0.14 (0.17)	0.06 (0.16)	0.07 (0.16)	0.04 (0.16)	−0.38 (**<0.001**)	−0.40 (**<0.001**)	0.07 (0.59)
Right cerebellar lobule 6	18, −62, −20	57	3.88	0.08 (0.19)	0.02 (0.16)	0.03 (0.16)	0.00 (0.16)	−0.32 (**0.002**)	−0.27 (**0.01**)	−0.19 (0.10)
Right cerebellar lobule 4–5	20, −42, 22		3.5							
Right hippocampus	28, −36, −2	9	3.87	0.24 (0.24)	0.15 (0.21)	0.17 (0.20)	0.10 (0.21)	−0.34 (**<0.001**)	−0.27 (**0.01**)	−0.29 (**0.01**)
Left superior occipital gyrus	−14, −96, 8	40	3.84	0.23 (0.22)	0.14 (0.21)	0.17 (0.20)	0.09 (0.22)	−0.34 (**<0.001**)	−0.26 (**0.02**)	−0.30 (**0.02**)
Left inferior occipital gyrus	−34, −88, −10	36	3.67	0.29 (0.25)	0.20 (0.22)	0.23 (0.22)	0.15 (0.21)	−0.30 (**0.003**)	−0.21 (**0.048**)	−0.38 (**0.001**)
Left middle occipital gyrus	−46, −74, 2	25	3.57	0.23 (0.22)	0.14 (0.21)	0.16 (0.20)	0.10 (0.20)	−0.39 (**<0.001**)	−0.31 (**0.005**)	−0.30 (**0.01**)
Right lingual gyrus	22, −90, −6	49	3.57	0.25 (0.27)	0.15 (0.22)	0.17 (0.22)	0.11 (0.22)	−0.32 (**0.002**)	−0.28 (**0.01**)	−0.18 (0.10)
Right calcarine sulcus	16, −98, −4		3.21							
Right parahippocampal gyrus	28, −18, −22	12	3.47	0.12 (0.20)	0.04 (0.18)	0.06 (0.18)	0.02 (0.18)	−0.32 (**0.002**)	−0.28 (**0.01**)	−0.16 (0.18)
Right inferior occipital gyrus	32, −78, −8	30	3.46	0.23 (0.23)	0.16 (0.19)	0.18 (0.20)	0.12 (0.17)	−0.29 (**0.004**)	−0.21 (**0.048**)	−0.33 (**0.002**)
Left paracentral lobule	−12, −32, 74	7	3.4	0.28 (0.26)	0.19 (0.24)	0.20 (0.24)	0.16 (0.24)	−0.31 (**0.002**)	−0.28 (**0.01**)	−0.14 (**0.02**)
Right-hand motor network										
Left calcarine sulcus	−16, −50, 8	11	4.4	0.12 (0.20)	0.05 (0.16)	0.05 (0.16)	0.04 (0.16)	−0.34 (**<0.001**)	−0.32 (**0.003**)	−0.10 (0.34)
Left paracentral lobule	−4, −36, 74	84	3.78	0.28 (0.25)	0.19 (0.21)	0.20 (0.22)	0.16 (0.19)	−0.36 (**<0.001**)	−0.31 (**0.005**)	−0.22 (**0.04**)
Right precuneus	6, −44, 66		3.62							
Left precuneus	−2, −38, 60		3.26							

(Continued)

Table 3. (Continued)

Region	MNI coordinates	kE	*T* value	HC Mean (SD)	MS Mean (SD)	RRMS Mean (SD)	PMS Mean (SD)	MS vs HC ES (p_{FDR})	RRMS vs HC ES (p_{FDR})	PMS vs RRMS ES (p_{FDR})
Left cerebellar lobule 4–5	−4, −54, −8	5	3.4	0.09 (0.15)	0.03 (0.18)	0.04 (0.19)	0.007 (0.17)	−0.42 (**<0.001**)	−0.41 (**<0.001**)	−0.02 (0.89)
Left cerebellum crus 2	−2, −74, −38	7	3.35	0.09 (0.18)	0.03 (0.19)	0.04 (0.19)	−0.009 (0.18)	−0.35 (**<0.001**)	−0.28 (**0.01**)	−0.27 (**0.04**)
Increased RS FC in MS patients compared to HC										
Left-hand motor network										
Right inferior frontal gyrus	56, 6, 8	129	4.46	0.05 (0.16)	0.12 (0.15)	0.12 (0.14)	0.12 (0.16)	0.43 (**<0.001**)	0.42 (**<0.001**)	0.06 (0.62)
Left supramarginal gyrus	−62, 22, 28	47	4.43	0.04 (0.18)	0.11 (0.19)	0.10 (0.19)	0.13 (0.20)	0.41 (**<0.001**)	0.36 (**0.002**)	0.21 (0.15)
Right superior temporal gyrus	58, −30, 22	245	4.37	0.04 (0.19)	0.11 (0.17)	0.11 (0.17)	0.12 (0.18)	0.42 (**<0.001**)	0.38 (**<0.001**)	0.14 (0.27)
Right supramarginal gyrus	60, −24, 32		4.35							
Right precuneus	14, −44, 46	77	3.99	0.06 (0.15)	0.14 (0.15)	0.13 (0.14)	0.15 (0.15)	0.51 (**<0.001**)	0.47 (**<0.001**)	0.15 (0.24)
Left inferior frontal gyrus	−52, 4, 8	30	3.9	0.05 (0.18)	0.11 (0.16)	0.10 (0.16)	0.11 (0.17)	0.35 (**<0.001**)	0.33 (**0.002**)	0.07 (0.53)
Right precentral gyrus	46, 4, 46	14	3.76	0.05 (0.15)	0.12 (0.15)	0.11 (0.15)	0.13 (0.16)	0.49 (**<0.001**)	0.46 (**<0.001**)	0.10 (0.45)
Right middle cingulum	8, 8, 38	42	3.73	0.06 (0.18)	0.14 (0.17)	0.13 (0.17)	0.16 (0.18)	0.40 (**<0.001**)	0.36 (**0.001**)	0.15 (0.24)
Left middle cingulum	−8, 8, 38	37	3.66	0.05 (0.18)	0.11 (0.16)	0.11 (0.16)	0.13 (0.16)	0.37 (**<0.001**)	0.36 (**0.001**)	0.04 (0.74)
Right-hand motor network										
Left inferior frontal gyrus	−52, 4, 8	175	5.39*	0.06 (0.15)	0.13 (0.15)	0.13 (0.16)	0.14 (0.15)	0.49 (**<0.001**)	0.48 (**<0.001**)	0.07 (0.57)
Right inferior frontal gyrus	56, 6, 14	169	4.8	0.06 (0.15)	0.13 (0.16)	0.13 (0.16)	0.11 (0.14)	0.46 (**<0.001**)	0.50 (**<0.001**)	−0.16 (0.21)
Right superior temporal gyrus	50, −36, 20	78	4.45	0.04 (0.14)	0.10 (0.15)	0.11 (0.15)	0.08 (0.15)	0.46 (**<0.001**)	0.51 (**<0.001**)	−0.16 (0.23)
Right supramarginal gyrus	42, −34, 24		4.01							
Left supramarginal gyrus	−62, −22, 26	41	4.35	0.05 (0.18)	0.11 (0.19)	0.12 (0.18)	0.14 (0.20)	0.43 (**<0.001**)	0.40 (**<0.001**)	0.18 (0.20)
Left superior temporal gyrus	−60, −40, −20	30	3.69	0.04 (0.16)	0.09 (0.16)	0.10 (0.16)	0.09 (0.15)	0.40 (**<0.001**)	0.39 (**<0.001**)	0.02 (0.89)

HC: healthy controls; MS: multiple sclerosis; RRMS: relapsing-remitting MS; PMS: progressive MS; SD: standard deviation; ES: effect size; FDR: false discovery rate; kE: cluster extent; MNI: Montreal Neurological Institute; RS: resting state; FC: functional connectivity. Statistically significant results are highlighted in bold.
*Clusters surviving at $p < 0.05$, family-wise error (FWE) corrected for multiple comparisons.

Table 4. Informative MRI predictors of the Expanded Disability Status Scale (EDSS) score, right and left nine-hole peg tests (9HPT) and right and left electronic finger tapping rate tests (EFTR) in MS patients, selected with random forest analyses, ordered by their relative importance ($p < 0.05$).

Predictor	Relative importance	*p*
EDSS (OOB-R2 = 0.71, OOB-MSE = 0.29)		
Normalized brain volume	100.0	<0.001
Normalized gray matter volume	78.7	<0.001
Cerebellar gray matter component I	62.1	0.002
Right inferior cerebellar peduncle FA	50.7	0.002
Basal ganglia gray matter component	35.1	0.01
Cerebellar gray matter component IV	34.0	0.005
Left middle cerebellar peduncle FA	30.5	0.01
Left inferior cerebellar peduncle FA	28.6	0.01
Cerebellar gray matter component III	28.5	0.01
Right corticospinal tract FA	26.4	0.01
T2-lesion volume	24.9	0.01
T1-lesion volume	23.8	0.02
Corpus callosum body MD	21.8	0.02
Sensorimotor gray matter component III	20.6	0.02
Corpus callosum FA	20.1	0.01
Right middle cerebellar peduncle FA	19.5	0.02
Right z9HPT (OOB-R2 = 0.36, OOB-MSE = 0.64)		
Right inferior cerebellar peduncle FA	100.0	0.006
Normalized brain volume	96.3	0.01
Normalized gray matter volume	84.2	0.02
Cerebellar gray matter component III	73.2	0.01
Right inferior cerebellar peduncle MD	58.6	0.01
Cerebellar gray matter component IV	50.4	0.04
Cerebellar gray matter component I	42.8	0.04
Left z9HPT (OOB-R2 = 0.38, OOB-MSE = 0.62)		
T1-lesion volume	100.0	<0.001
Left inferior cerebellar peduncle FA	73.6	0.004
T2-lesion volume	64.7	0.004
Normalized brain volume	54.6	0.005
Corpus callosum body FA	49.3	0.005
Corpus callosum body MD	46.1	0.006
Left superior cerebellar peduncle FA	42.8	0.006
Normalized gray matter volume	39.2	0.02
Sensorimotor gray matter component III	32.3	0.03
Left middle cerebellar peduncle FA	32.0	0.04
Left inferior cerebellar peduncle MD	28.4	0.02
Left superior cerebellar peduncle MD	26.7	0.02
Right zEFTR (OOB-R2 = 0.18, OOB-MSE = 0.82)		
Normalized gray matter volume	100.0	0.004
Sensorimotor gray matter component I	52.5	0.03
Cerebellar gray matter component IV	41.2	0.04
Right inferior cerebellar peduncle MD	29.3	0.048
Left zEFTR (OOB-R2 = 0.22, OOB-MSE = 0.78)		
Left inferior cerebellar peduncle FA	100.0	0.007
Left middle cerebellar peduncle FA	95.6	0.009

(Continued)

Table 4. (Continued)

Predictor	Relative importance	p
Normalized gray matter volume	85.4	0.01
Cerebellar gray matter component IV	70.0	0.01
Sensorimotor gray matter component I	68.0	0.01
Normalized brain volume	60.4	0.04
Cerebellar gray matter component III	54.2	0.03
Left superior cerebellar peduncle FA	49.2	0.01

EDSS: Expanded Disability Status Scale; 9HPT: nine-hole peg test; EFTR: electronic finger tapping rate test; OOB: out of bag; OOB-MSE: out of bag mean squared error, prediction error on the out-of-bag observations; FA: fractional anisotropy; MD: mean diffusivity; RS: resting state; FC: functional connectivity.

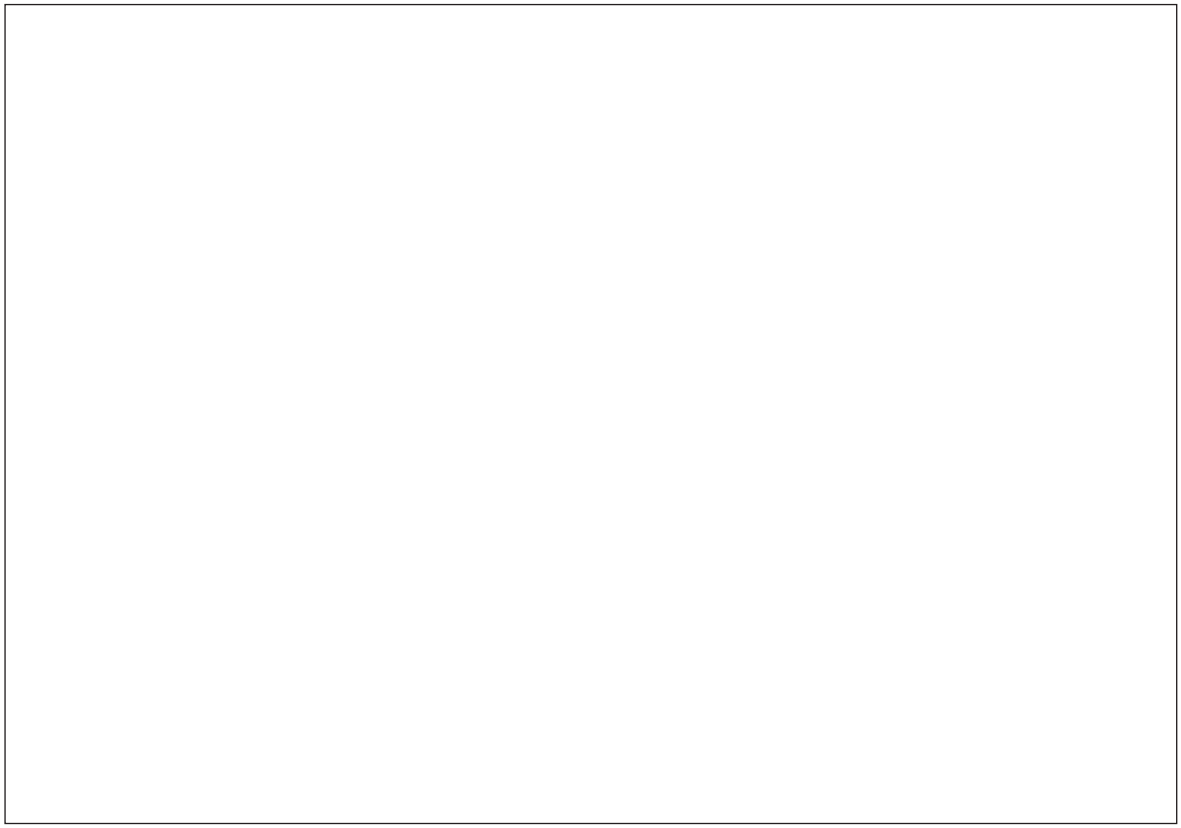

Figure 3. Informative MRI predictors of global disability and impaired hand performance in multiple sclerosis patients.
Bar charts showing relative importance of MRI predictors of Expanded Disability Status Scale (EDSS) score, right and left nine-hole peg tests (9HPT) and right and left electronic finger tapping rate tests (EFTR) in multiple sclerosis (MS) patients, selected with random forest analyses (p 0.05). Bar colors reflect the magnitude of Spearman's correlation of each predictor with the outcome.
EDSS: Expanded Disability Status Scale; GM: gray matter; ICP: inferior cerebellar peduncle; FA: fractional anisotropy; CC: corpus callosum; MCP: middle cerebellar peduncle; CST: corticospinal tract; LV: lesion volume; MD: mean diffusivity; z9HPT: nine-hole peg test z-score; SCP: superior cerebellar peduncle; zEFTR: electronic finger tapping rate test z-score.

only predictors of global disability but also those of hand-motor impairment. Interestingly, for both these analyses, atrophy of the basal ganglia network emerged among the best predictors of clinical impairment. This is consistent with the early neurodegenerative phenomena occurring at this level, as supported by volumetric studies performed in patients at different stages of the disease.[29] In patients with PMS, significant predictors were identified only for EDSS score and included atrophy of sensorimotor and cerebellar networks, damage to

Table 5. Informative MRI predictors of the Expanded Disability Status Scale (EDSS) score, right and left nine-hole peg tests (9HPT) and right and left electronic finger tapping rate tests (EFTR) in RRMS and PMS patients, selected with random forest analyses, ordered by their relative importance ($p < 0.05$).

Predictors in RRMS patients	Relative importance	*p*
EDSS (OOB-R2 = 0.19, OOB-MSE = 0.81)		
Basal ganglia gray matter component	100.0	<0.001
Normalized brain volume	98.9	<0.001
Normalized gray matter volume	43.0	0.01
Corpus callosum body MD	42.4	0.009
Corpus callosum body FA	38.2	0.02
Right middle cerebellar peduncle FA	34.6	0.02
Left middle cerebellar peduncle FA	31.5	0.03
T2-lesion volume	30.7	0.02
Right inferior cerebellar peduncle FA	26.3	0.047
Left superior cerebellar peduncle MD	22.8	0.04
Cerebellar gray matter component I	19.1	0.047
Right z9HPT (OOB-R2 = 0.14, OOB-MSE = 0.86)		
Normalized gray matter volume	100.0	0.008
T2-lesion volume	77.1	<0.001
Left Cingulum FA	71.3	0.01
Normalized brain volume	69.7	0.02
Right inferior cerebellar peduncle FA	62.5	0.03
T1-lesion volume	56.0	0.02
Cerebellar gray matter component I	42.6	0.02
Left z9HPT (OOB-R2 = 0.24, OOB-MSE = 0.76)		
Left inferior cerebellar peduncle FA	100.0	<0.001
T1-lesion volume	75.4	0.004
Basal ganglia gray matter component	74.8	0.003
T2-lesion volume	68.9	0.001
Corpus callosum body MD	65.9	0.003
Left superior cerebellar peduncle MD	60.4	0.006
Corpus callosum body FA	49.0	0.02
Left inferior cerebellar peduncle MD	39.3	0.01
Left middle cerebellar peduncle MD	31.8	0.03
Predictor in PMS patients	**Relative importance**	***p***
EDSS (OOB-R2 = 0.16, OOB-MSE = 0.84)		
Cerebellar gray matter component I	100.0	0.02
Sensorimotor gray matter component II	97.3	0.02
Left inferior cerebellar peduncle FA	85.8	0.03
Increased RS FC right inferior frontal gyrus(Left-hand RS network)	65.1	0.04

EDSS: Expanded Disability Status Scale; 9HPT: nine-hole peg test; EFT: electronic finger tapping rate test; OOB: out of bag; OOB-MSE: out of bag mean squared error, prediction error on the out-of-bag observations; FA: fractional anisotropy; MD: mean diffusivity; RS: resting state; FC: functional connectivity.

the left inferior cerebellar peduncle and increased RS FC between left-hand motor cortex and IFG. All together, these limited numbers of variables explained only a minimal part of global disability (16%), indicating that other factors, not included in our analysis, such as spinal cord damage and cortical lesions might be at work to explain clinical impairment in this phenotype.[30,31] Interestingly, no measure of global damage emerged in this analysis, which might be due to a plateau effect of the accumulation of widespread

structural damage. All these aspects could negatively influence the identification of univocal and clear predictors of impaired motor performance in PMS patients.

The importance of atrophy of the sensorimotor and cerebellar networks for global clinical disability in patients with PMS is in line with several previous studies[32–34] and with the trajectory of atrophy spreading from deep GM structures to cortical GM areas described over the course of the disease.[29] In PMS, in addition to measures of structural damage to motor-related regions, also increased RS FC between left-hand motor cortex and right IFG contributed to explain clinical disability. This is a key area of the mirror-neuron system and modulation of its RS FC was found to underlie clinical improvements following upper-limb rehabilitation in MS.[18,35] Moreover, a previous active fMRI study showed that PMS patients experienced greater activation of frontal areas like the IFG during a simple upper-limb motor task, supporting the hypothesis that in advanced disease stages the exhaustion of brain-adaptive mechanisms might result in the involvement of previously silent second-order compensatory areas, which however contributes to disability accumulation.[13]

This study is not without limitations. First, it is cross-sectional. This allowed us to include a very large number of cases. However, longitudinal observations are needed to define the dynamic interplay between evolution of clinical deficits in the different phases of the disease and the accumulation of structural and functional MRI abnormalities in the CNS. Second, to have informative data on a large number of patients (including both RRMS and PMS), we performed an a priori selection of techniques and structures to include in the prediction models. Clearly, we cannot exclude that the analysis of other variables (e.g. spinal cord, cortical lesions) or MRI methods (focused entirely on upper-limb motor regions) would have resulted in better classification models. Moreover, other upper-limb measures (e.g. Pinch and Jamar dynamometers or Action-Research Arm Test) as well as lower limbs ones could be used to provide a more comprehensive and specific assessment of limb motor function. Finally, cognitive impairment should be taken into account in future studies to better discriminate the motor-specific substrates of upper-limb motor performance.

In conclusion, global measures of atrophy and lesions as well as measures of structural damage of motor-related regions contribute to explain motor impairment in RRMS, whereas in PMS also increased RS FC between hand-motor cortex of non-dominant hemisphere and homolateral IFG significantly influence clinical disability. Multiparametric MRI approaches could be relevant to investigate the substrates of motor impairment in different MS phenotypes.

Authors' Contributions

M.A.R. contributed to the conception and design of the study. C.C., A.M., P.V., F.E., E.P., M.F., and M.A.R. contributed to the acquisition and analysis of data. C.C., M.H.d.l.C., A.M., P.V., and M.A.R. contributed to drafting the text and preparing the figures.

Declaration of Conflicting Interests

The author(s) declared the following potential conflicts of interest with respect to the research, authorship, and/or publication of this article: C.C., M.H.d.l.C., and F.E. have nothing to report. E.P., A.M., and P.V. received speaker honoraria from Biogen Idec. M.F. is Editor-in-Chief of the *Journal of Neurology*; received compensation for consulting services and/or speaking activities from Bayer, Biogen Idec, Merck-Serono, Novartis, Roche, Sanofi Genzyme, Takeda, and Teva Pharmaceutical Industries; and receives research support from Biogen Idec, Merck-Serono, Novartis, Roche, Teva Pharmaceutical Industries, Italian Ministry of Health, Fondazione Italiana Sclerosi Multipla, and ARiSLA (Fondazione Italiana di Ricerca per la SLA). M.A.R. received speaker honoraria from Biogen Idec, Novartis, Teva Neurosciences, Merck-Serono, Genzyme, Roche, Bayer, and Celgene and receives research support from the Canadian MS Society and Fondazione Italiana Sclerosi Multipla.

Funding

The author(s) disclosed receipt of the following financial support for the research, authorship, and/or publication of this article: This study has been partially supported by FISM—Fondazione Italiana Sclerosi Multipla—cod. 2018/S/3 and financed or co-financed with the "5 per mille" public funding.

ORCID iDs

Claudio Cordani https://orcid.org/0000-0002-9014-7887
Milagros Hidalgo de la Cruz https://orcid.org/0000-0002-7574-2143
Massimo Filippi https://orcid.org/0000-0002-5485-0479
Maria A Rocca https://orcid.org/0000-0003-2358-4320

Supplemental Material

Supplemental material for this article is available online.

References

1. Yozbatiran N, Baskurt F, Baskurt Z, et al. Motor assessment of upper extremity function and its relation with fatigue, cognitive function and quality of life in multiple sclerosis patients. *J Neurol Sci* 2006; 246: 117–122.
2. Kister I, Chamot E, Salter AR, et al. Disability in multiple sclerosis: A reference for patients and clinicians. *Neurology* 2013; 80: 1018–1024.
3. Kurtzke JF. Rating neurologic impairment in multiple sclerosis: An expanded disability status scale (EDSS). *Neurology* 1983; 33(11): 1444–1452.
4. Lamers I, Kelchtermans S, Baert I, et al. Upper limb assessment in multiple sclerosis: A systematic review of outcome measures and their psychometric properties. *Arch Phys Med Rehabil* 2014; 95(6): 1184–1200.
5. Feys P, Lamers I, Francis G, et al. The nine-hole peg test as a manual dexterity performance measure for multiple sclerosis. *Mult Scler* 2017; 23(5): 711–720.
6. Ruff RM and Parker SB. Gender- and age-specific changes in motor speed and eye-hand coordination in adults: Normative values for the finger tapping and grooved pegboard tests. *Percept Mot Skills* 1993; 76(3 Pt. 2): 1219–1230.
7. Cattaneo D, Lamers I, Bertoni R, et al. Participation restriction in people with multiple sclerosis: Prevalence and correlations with cognitive, walking, balance, and upper limb impairments. *Arch Phys Med Rehabil* 2017; 98(7): 1308–1315.
8. Solaro C, Cattaneo D, Brichetto G, et al. Clinical correlates of 9-hole peg test in a large population of people with multiple sclerosis. *Mult Scler Relat Disord* 2019; 30: 1–8.
9. Filippi M, Preziosa P, Langdon D, et al. Identifying progression in multiple sclerosis: New perspectives. *Ann Neurology* 2020; 88: 438–452.
10. Ceccarelli A, Rocca MA, Pagani E, et al. A voxel-based morphometry study of grey matter loss in MS patients with different clinical phenotypes. *Neuroimage* 2008; 42: 315–322.
11. Cortese R, Collorone S, Ciccarelli O, et al. Advances in brain imaging in multiple sclerosis. *Ther Adv Neurol Disord* 2019; 12: 1756286419859722.
12. Rocca MA, Valsasina P, Leavitt VM, et al. Functional network connectivity abnormalities in multiple sclerosis: Correlations with disability and cognitive impairment. *Mult Scler* 2018; 24(4): 459–471.
13. Rocca MA, Colombo B, Falini A, et al. Cortical adaptation in patients with MS: A cross-sectional functional MRI study of disease phenotypes. *Lancet Neurol* 2005; 4(10): 618–626.
14. D'Ambrosio A, Pagani E, Riccitelli GC, et al. Cerebellar contribution to motor and cognitive performance in multiple sclerosis: An MRI sub-regional volumetric analysis. *Mult Scler* 2017; 23(9): 1194–1203.
15. Cordani C, Meani A, Esposito F, et al. Imaging correlates of hand motor performance in multiple sclerosis: A multiparametric structural and functional MRI study. *Mult Scler* 2019: 1352458518822145.
16. Oldfield RC. The assessment and analysis of handedness: The Edinburgh inventory. *Neuropsychologia* 1971; 9(1): 97–113.
17. Xu L, Groth KM, Pearlson G, et al. Source-based morphometry: The use of independent component analysis to identify gray matter differences with application to schizophrenia. *Hum Brain Mapp* 2009; 30(3): 711–724.
18. Rocca MA, Meani A, Fumagalli S, et al. Functional and structural plasticity following action observation training in multiple sclerosis. *Mult Scler* 2019; 25(11): 1472–1487.
19. Benjamini YHY. Controlling the false discovery rate: A practical and powerful approach to multiple testing. *J Royal Stat Soc Series B* 1995; 57: 289–300.
20. Breiman L. Random forest. *Mach Learn* 2001; 45: 5–32.
21. Efron B and Tibshirani R. Improvements on cross-validation: The .632_ bootstrap method. *J Am Stat Assoc* 1997; 92: 548–560.
22. Altmann A, Tolosi L, Sander O, et al. Permutation importance: A corrected feature importance measure. *Bioinformatics* 2010; 26: 1340–1347.
23. Preziosa P, Rocca MA, Mesaros S, et al. Relationship between damage to the cerebellar peduncles and clinical disability in multiple sclerosis. *Radiology* 2014; 271(3): 822–830.
24. Peterson DS and Fling BW. How changes in brain activity and connectivity are associated with motor performance in people with MS. *Neuroimage Clin* 2018; 17: 153–162.
25. Gera G, Fling BW and Horak FB. Cerebellar white matter damage is associated with postural sway deficits in people with multiple sclerosis. *Arch Phys Med Rehabil* 2020; 101(2): 258–264.
26. Jueptner M and Weiller C. A review of differences between basal ganglia and cerebellar control of movements as revealed by functional imaging studies. *Brain* 1998; 121(Pt. 8): 1437–1449.

27. Bonzano L, Tacchino A, Roccatagliata L, et al. Structural integrity of callosal midbody influences intermanual transfer in a motor reaction-time task. *Hum Brain Mapp* 2011; 32(2): 218–228.

28. Cerqueira JJ, Compston DAS, Geraldes R, et al. Time matters in multiple sclerosis: Can early treatment and long-term follow-up ensure everyone benefits from the latest advances in multiple sclerosis. *J Neurol Neurosurg Psychiatry* 2018; 89(8): 844–850.

29. Eshaghi A, Marinescu RV, Young AL, et al. Progression of regional grey matter atrophy in multiple sclerosis. *Brain* 2018; 141: 1665–1677.

30. Calabrese M, Rocca MA, Atzori M, et al. Cortical lesions in primary progressive multiple sclerosis: A 2-year longitudinal MR study. *Neurology* 2009; 72: 1330–1336.

31. Rocca MA, Preziosa P and Filippi M. Application of advanced MRI techniques to monitor pharmacologic and rehabilitative treatment in multiple sclerosis: Current status and future perspectives. *Expert Rev Neurother* 2019; 19(9): 835–866.

32. Sailer M, Fischl B, Salat D, et al. Focal thinning of the cerebral cortex in multiple sclerosis. *Brain* 2003; 126(Pt. 8): 1734–1744.

33. Charil A, Dagher A, Lerch JP, et al. Focal cortical atrophy in multiple sclerosis: Relation to lesion load and disability. *Neuroimage* 2007; 34: 509–517.

34. Petracca M, Margoni M, Bommarito G, et al. Monitoring progressive multiple sclerosis with novel imaging techniques. *Neurol Ther* 2018; 7(2): 265–285.

35. Cordani C, Valsasina P, Preziosa P, et al. Action observation training promotes motor improvement and modulates functional network dynamic connectivity in multiple sclerosis. *Mult Scler*. Epub ahead of print 5 November 2019. DOI: 10.1177/1352458519887332.